ANALYTICAL MODEL OF FLAME SPREAD IN FULL-SCALE ROOM/CORNER TESTS (ISO9705)

Mark Dietenberger, USDA Forest Service, Forest Products Laboratory, Madison, Wisconsin*
and Ondrej Grexa, State Forest Products Research Institute, Bratislava, Slovak Republic

ABSTRACT

A physical, yet analytical, model of fire growth has predicted flame spread and rate of heat release (RHR) for an ISO9705 test scenario using bench-scale data from the cone calorimeter. The test scenario simulated was the propane ignition burner at the comer with a 100/300 kW program and the specimen lined on the walls only. Four phases of fire growth were simulated. The first two phases, the wall ignition and upward flame spread, have separate physical formulations. Some empiricism, however, was required to predict the phases of lateral and downward flame spread. Two groups of materials seem to exist that have different characteristics of lateral flame spread. The first group, containing the heavy composite boards, displayed a continuously increasing RHR along with accelerating flame spread. The second group, which contains plywoods and lumbers, have a constant or decreasing RHR while in a slow flame spreading mode. The analytical model has predicted sensitivity of RHR to various systematic measurement errors. Disagreements about RHR at flashover were predicted as a result of differing gas analysis systems between laboratories. Delay of wall ignition due to differing sluggishness of the burner between laboratories was predicted. Other results with burner program and upper gas layer mixing are reported.

BACKGROUND

Two analytical models for room fire growth were found with a literature search. The first is by Wickstrom and Goransson[1] in which the cone calorimeter data are used as input to a simplified fire growth model. The second model by Karlson[2] takes a more physically reasonable approach by extending the model of Saito and others[3] (SQW) for thermal modeling of upward spread on a wall to a thermal model of flame spread along the ceiling lining. After the initial phases of wall and ceiling ignitions, the flame spread model uses a decaying heat release flux profile coupled with the flame spread rate formula to analytically simulate accelerating, oscillating, or decaying fire growth behavior. Neither of the models is applicable to the test scenario with test materials on the wall only.

The four significant stages of fire growth leading to flashover are back wall ignition, upward flame spread to the ceiling, lateral-ceiling flame spread nearly to the ends of the room, and finally, a rapid uniform downward flame spread just prior to flashover[4,5]. A numerical model covering all four phases (modification of Quintiere's model[6]) to predict a fire growth scenario for use on a personal computer was described previously by Janssens and others[7]. Some first order differential equations were set up to simulate specific events such as upward, lateral, and downward flame spread while including material burnout, approximated radiation from upper gas layer, and temperature responses of wall lining and upper gas layers. However, there were also limitations to this and other recent models.

Evaluation of recent experimental data suggests some simple formulations of submodels for the room fire growth model. The average surface heat flux within the initial ignition area has been measured with fluxmeters at around 55 kW/m^2 for the burner's RHR from 40 to 300 kW for both ISO and ASTM burner[8,9] (also our facility). At the flame height, the total heat flux already decreases to about 25 kW/m^2 and continues to decrease similarly to a decaying exponential function. A real material would have even lower surface heat flux because a surface temperature approaching the pyrolysis temperature would lower flame heat flux and increase the surface re-radiating cooling flux. Similar adjustments to surface heat flux will also be required in the cone calorimeter test conditions. With the gypsum board as a back board to testing materials, recent cone calorimeter tests show that the secondary peak RHR often noted for wood-based materials is significantly reduced and extends for longer period of time (even up to 20 minutes) due to heat losses into the back board. Thus, the exponentially decaying RHR profile in the Karlson model would be more realistic than the modified Quintiere model's constant RHR and then sharp drop of RHR at burnout time.

In detailed measurements by Kulkarni and others[10] of upward flame propagation on finitely thick materials exposed to external flux, the flame flux profile follows a decaying exponential form immediately at the pyrolysis front. However, in the analytical model, all the surface heat fluxes are incorporated into the "flame flux profile" to completely avoid calculation of preheat temperatures[11] and thus maintain the simplicity of the model for the ISO9705 test conditions. One might assert that preheat temperatures due to radiation from the upper hot gas layer need to be calculated just prior to flashover to create the accelerating RHR profile typically observed. However, an actual RHR that uniformly increases with time in the room will be observed as an accelerating profile because the RHR measurements are affected significantly by the gas mixing time responses in the gas train and in the room's upper gas layer. Secondly, it is possible to evaluate radiation view factors from the bottom surface of the hot smoky gas layer to the walls so that a flame flux profile is formulated for the downward flame spread. The analytical model developed here will actually demonstrate these effects, and then their importance can be assessed.

MODEL FORMULATION

Wall Ignition Phase

In the analysis for ignition, we used the ignitability parameters derived from the cone calorimeter data. Since the imposed heat flux is from the propane burner rather than the cone heater, the equation for surface heat flux being absorbed into the surface (fluxmeter or material) is

$$\dot{q}''_w = \varepsilon_m \sigma (\varepsilon_f T_f^4 - T_m^4) + h_c (T_f - T_m) \qquad [1]$$

The parameters that are known in the case of fluxmeters are $\dot{q}''_w = 55\ kW/m^2$, $T_m = 298\ K$, and $\varepsilon_m = 0.97$. Three remaining parameters are properties of the propane flame only. The temperature rise above ambient of the propane flame above the ignition area has been measured at about 880ºC by Hasemi[12], 959ºC by Kokkala and Heinila[8], and 754ºC by Janssens and Tran[13]. Most revealing are the contour plots of flame temperatures at 30 mm from the surface by Kokkala and Heinila[8] in which the contour of 900ºC covers a reasonably sized ignition area for various burner sizes and output. With these considerations and using the flame temperature $T_f = 1173\ K$, we obtain the high but still reasonable values of flame emissivity and convective coefficient of $\varepsilon_f = 0.395$ and $h_c = 0.0165$ kW / m^2K to match the heat flux observed with the fluxmeters. The heat loss flux to ambient in which the steady state surface temperature is the ignition temperature is given by

$$\dot{q}''_{ig} = \varepsilon_m \sigma (T_{ig}^4 - T_m^4) + h_c (T_{ig} - T_m) = h_{ig} (T_{ig} - T_m) \qquad [2]$$

The Janssens[14] correlation for time to ignition has good accuracy for the heat flux ratios from 1 to 10 and Fourier number, $kt_{ig} / C\rho\delta_m^2$, less than 0.33, which are expected for our room tests. His analytic expression for time to ignition is

$$t_{ig,0} = \frac{k\rho C_p}{h_{ig}^2}\left(\frac{0.73}{\dot{q}''_w / \dot{q}''_{ig} - 1}\right)^{\frac{1}{0.547}} \quad [3]$$

Suppose the imposed flux from the burner has the sluggish response as in (and showing the Duhamel's convolution integral equivalent)

$$\dot{q}''_b(t) \equiv \dot{q}''_w S_b(t) \equiv \dot{q}''_w(1 - \exp(-t/\tau_b)) = \int_0^t \frac{\dot{q}''_w}{\tau_b}\exp(-(t-\xi)/\tau_b)\mathrm{d}\xi \equiv \dot{q}''_w \otimes \dot{S}_b \quad [4]$$

The effect of a sluggish burner on the classical surface temperature rise is analyzed with the Duhamel's supposition integral and solved by the Laplace transform method with the result

$$\sqrt{\pi k\rho c}\,\frac{T_s - T_m}{2\dot{q}''_w} = \frac{1}{2\sqrt{t}} \otimes S_b(t) = \sqrt{t} \otimes \dot{S}_b = \sqrt{t} - \sqrt{\tau_b}\exp\left(\frac{-t}{\tau_b}\right)\int_0^{\sqrt{t/\tau_b}} \exp(\lambda^2)\mathrm{d}\lambda \quad [5]$$

The result is the appearance of the Dawson function as the exponential-integral term, and its evaluation is available in the literature as an accurate functional relationship. The square root of the right side of Equation [3] is approximately proportional to the temperature rise to the ignition point for typical times to ignition. Therefore, we can apply Equation [5] to delay the time to ignition as in

$$\sqrt{t_{ig,0}} = \sqrt{t_{ig}} - \sqrt{\tau_b}\,Dawson(t_{ig}/\tau_b) \quad [6]$$

This nonlinear function was solved by an interval-halving method rather than the standard Newton-Raphson method to ensure rapid and correct convergence. To use Equation [3], the material properties of thermal conductivity, volumetric heat capacity, surface emissivity, and surface temperature at ignition are required. These properties were determined using the method by Dietenberger[15]. Derived material property values for Equations [1] to [3] are listed in Tables 1 and 2. Using Equation [6] for the room test materials, the range of time to ignitions in the case of instant burner response, $\tau_b = 0$, is from 8.4 seconds for the oak-veneer plywood to 23 seconds for the particle board. Setting the burner time constant to 1 and 6 seconds, respectively, generally increases the time to ignition by 1.03 seconds and 6.7 seconds, respectively. It has been shown that a burner's time constant of 6 seconds is enough to account for the increase in time to ignition indicated by Karlson[2]. That is, Karlson found the time to ignition on the wall to correlate best with the cone heater flux of 50 kW/m^2, providing a multiplication factor of 1.7 times the time to ignition from the cone calorimeter data was used. Even if this may not be a problem with the data used by Karlson, the effect of not knowing the propane burner response can be a significant source of confusion and error in ignitability in room tests between laboratories or even within a laboratory if quality control is not maintained. Because of our use of the electronic mass flow controller, we only expect a 1-second delay in the time to ignition. This was found to be consistent with our existing data on the time to ignition of the wall.

Formulation for Rate of Flame Spread

The next three phases of fire growth are similar in that they involve the flame spreading process. The first step of the analysis is to describe the extended flame flux profile as an imposed flux applied over the distance, y_c, followed by an exponential decay with characteristic length, δ_f, as in

$$\dot{q}''_{wf}(y) = \dot{q}''_w\left[H(y) + \left(\exp\left\{\frac{-(y-y_c)}{\delta_f}\right\} - 1\right)H(y-y_c)\right] \quad [7]$$

where $H(y)$ is the heavyside function. In the case where flame is only from the material burning, Kulkarni et al.[10] have found the characteristic length to be proportional to the extended flame length and correlated as $\delta_f = (yf - y_p) / c_f$, with value of c_f as 1.37. However, with the pilot burner

Table 1. Ignitability input parameters to analytical model.

Material	Test No.	$k/\rho C_p$ (m^2/s) $\times 10^7$	Material emissivity	$k\rho C_p$ (kJ^2/m^4K^2s)	T_{ig} (K)
Gypsum board, Type X	1	3.74	0.9	0.451	608.5
FRT Douglas-fir plywood	2	1.60	0.9	0.308	660.0
Oak veneer plywood	3	1.44	0.9	0.171	630.0
FRT plywood (Forintek)	4	1.57	0.9	0.373	645.8
Douglas-fir plywood (ASTM)	5	1.60	0.9	0.254	609.2
FRT polyurethane foam	6	14.6	0.68	0.02	689.0
Gypsum board, Type X	7	see test 1			
FRT South Pine plywood	8				
Douglas-fir plywood (MB)	9	1.60	0.9	0.259	599.0
Southern Pine plywood	10	1.57	0.88	0.335	595.6
Particleboard	11	3.79	0.88	1.09	529.7
Oriented strandboard	12	0.932	0.88	0.217	621.0
Hardboard	13	1.50	0.88	0.763	553.9
Redwood lumber	14	1.25	0.86	0.129	638.0
Gypsum board, Type X	15	see test 1			
White spruce lumber	16	1.63	0.88	0.214	630.7
Southern Pine boards	17	1.60	0.88	0.270	640.2
Waferboard	18	1.57	0.88	0.325	587.8

Table 2. Burning input parameters to analytical model.

Material	Test No.	PRHR intercept (kW/m^2)	PRHR slope (-)	THR intercept (kJ/m^2)	THR slope (s)	$T_{s,burn}$ K
Gypsum board, Type X	1	34.1	1.26	1,481	45.4	708.5
FRT Douglas-fir plywood	2	34.3	1.57	14,740	312.2	760
Oak veneer plywood	3	155.4	2.98	38,572	350.9	730
FRT plywood (Forintek)	4	-2.1	2.71	10,509	439.4	745.8
Douglas-fir plywood (ASTM)	5	86.7	2.71	52,583	170.9	709.2
FRT polyurethane foam	6	3.12	1.49	0.0	271.6	689
Gypsum board, Type X	7	see test 1				
FRT South Pine plywood	8					
Douglas-fir plywood (MB)	9	98.4	1.77	63,900	200	699
Southern Pine plywood	10	57.4	2.49	82,600	0.0	695.6
Particleboard	11	115.8	1.91	86,529	609.3	629.7
Oriented strandboard	12	118.2	1.88	73,115	247.4	721
Hardboard	13	121.5	1.134	84,227	108.7	653.9
Redwood lumber	14	71.9	2.37	85,538	389	738
Gypsum board, Type X	15	see test 1				
White spruce lumber	16	101.8	1.17	93,592	-18.8	730.7
Southern Pine boards	17	84.4	1.77	119,544	137	740.2
Waferboard	18	139.9	1.00	86,196	442	687.8

flames merging with the material flames in the ISO9705 test protocol, the more appropriate data to use is reported by Kokkala and Heininla[8]. Using their figures of the flame flux profiles for different burner sizes and outputs, we estimated that the values for the ratio of extended flame length over characteristic length would vary from 1.2 to 1.4. Having established flame heat flux profile, we analyzed for the quasi-steady speed of the pyrolysis front by simply using the equality, $y - y_{ig} = v_p(t_{ig} - t)$, in Equation [7] to represent the sliding movement of the imposed heat flux profile over a given spot until ignition is reached. With this substitution, the Duhamel's supposition integral is the convolution of the material's thermal response with the time changing imposed flux as

$$T_{ig} - T_m = \frac{d(T_s - T_m)}{dt} \otimes \dot{q}''_{wf}(v_p(t_{ig} - t) + y_{ig}) = (T_s - T_m) \otimes \frac{d\dot{q}''_{wf}(y_{ig} - v_p(t - t_{ig}))}{dt} \qquad [8]$$

where the integration is taken from zero to the time of ignition, t_{ig}, to correspond to ignition temperature, T_{ig}. To accommodate the approaching steady state condition, the cooling flux given by Equation [2] is subtracted from Equation [7] (replace T_{ig} by T_s in Equation [2]) for use in Equation [8]. The resulting complex solution[11] is greatly simplified by using the experimental results from Kulkarni et al.[10] to observe that $y_p = y_{ig} = y_c$ and $y_o - y_{ig} >> \delta_f$. The simplified formula is

$$v_p = \delta_f / \tau_m \qquad [9]$$

where for thermally thick materials, the material time constant is

$$\tau_{m,thick} = k\rho C_p \left(\frac{T_{ig} - T_m}{\dot{q}''_w - \dot{q}''_{ig}} \right)^2 \qquad [10]$$

and for thermally thin materials, the material time constant is instead

$$\tau_{m,thin} = \rho C_p \delta_m \left(\frac{T_{ig} - T_m}{\dot{q}''_w - \dot{q}''_{ig}} \right) \qquad [11]$$

An accurate but simple interpolation formula for the material time constant over the full thermal regime from thick to thin was derived by Dietenberger[11] with the result

$$\tau_m = \tau_{m,thick} \left(\frac{1}{2} + \sqrt{\frac{1}{4} + \left(\frac{\tau_{m,thick}}{\tau_{m,thin}} \right)^n} \right)^{\left(\frac{-2}{n} \right)} \qquad [12]$$

where the value $n = 13$ obtained for the polymethyl methacrylate (PMMA) material is assumed to apply for other materials.

Coefficients for Upward and Downward Flame Spread

The final parameter to model is the characteristic length of flame extension. We begin with the correlation from experimental data[13] for the visible flame height:

$$y_f = y_o + 0.0433 \left(\frac{\dot{Q}_t}{2w} \right)^{2/3} \qquad [13]$$

Since the arc length of the pyrolysis front is $2w$, Equation [13] is rearranged as the flame area:

$$A_f = 2w(y_f - y_o) = 0.0433(2w)^{1/3} \dot{Q}_t^{2/3} \qquad \textbf{[14]}$$

In the linearization of Equation [14] (required for analytic solution), a good reference point is the transition from upward to lateral flame spread at the flame height, $y_{fu} - y_o = 2.4 - 0.3 = 2.1$ *m*. Substitution into Equation [14] shows that the RHR at the reference point can be related as $Q_{tu} = 161\, A_{fu}$. The linear approximation to Equation [14] is then

$$A_f = A_{fu} + \frac{dA_f}{d\dot{Q}_t}(\dot{Q}_t - \dot{Q}_{tu}) = \left(1 - 161 \frac{dA_f}{d\dot{Q}_t}\right) A_{fu} + \frac{dA_f}{d\dot{Q}_t} \dot{Q}_t \qquad [15]$$

At first, it seems the derivative of the flame area should also be evaluated at the reference point. However, the flame area would be much too large at lower values of RHR, particularly at 40 kW for the ASTM burner and 100 kW for the ISO burner. With only a 23% increase in the derivative at the reference point, the formula for the flame area for use in the model becomes

$$A_f = \frac{A_{fu}}{5.6} + \frac{\dot{Q}_t}{196} \qquad [16]$$

In the case of the ASTM burner, where RHR is 40 kW and burner width is 0.3 m, the computed flame area impinged on the wall is 0.429 m^2. This converts to a flame length of 0.715 m compared with 0.71 m obtained with Equation [13]. Likewise, for the case of the ISO burner, where RHR is 100 kW and burner width is 0.17 m, the computed flame area is 0.638 m^2. This converts to a flame length of 1.88 m compared with 1.91 m obtained with Equation [13]. Returning lastly to the discussion after Equation [7] concerning the flame characteristic length, the coefficients *a, b, & c* are defined as follows:

$$2w\delta_f \equiv \frac{2w(y_f - y_o) - 2w(y_p - y_o)}{c_f} \equiv \frac{A_f - A_p}{c_f} = \frac{A_{fu}}{5.6c_f} + \frac{\dot{Q}_t}{196c_f} - \frac{A_p}{c_f} = a + c\dot{Q}_t + bA_p \qquad [17]$$

The model for during downward flame spread is based on a simple concept. The radiative flux profile developed at the flame front is due to the view factor of radiation from the bottom surface of the smoky hot upper gas layer to a narrow strip ahead of the flame front. Thus, the view factor to a narrow strip ahead of the flame edge from a perpendicularly finitely wide sheet of width ℓ is

$$F_{dx-\ell} = \frac{1}{2}\left(1 - \left(1 + (\ell / y)^2\right)^{-1/2}\right) \approx \frac{1}{2}\exp(-y / \ell) \qquad [18]$$

Considering the similarity with Equation [7], it is obvious to make the identification, $\ell = \delta_f$. Since the length of the flame edge is the length of the room, the coefficient *a* is merely the area of the radiating sheet for downward flame spread along one wall. Since there are three walls with downward flame spreading, the identification for the coefficients is

$$a = 3A_{roof} / c_f, \quad b = -a / A_{max}, \quad c = 0 \qquad [19]$$

The coefficient *b* is defined to allow for damping of fire growth as all of the material becomes involved. Finally, the material time constant is not changed because there is not a better estimate for the imposed heat flux at the flame front for downward flame spreading.

Analytical Solution of Flame Spread

By substituting Equation [17] into Equation [9], the result is the controlling equation for fire growth:

$$\frac{dA_p}{dt} = \frac{a + bA_p + c\dot{Q}_t}{\tau_m} \qquad [20]$$

where the total RHR is given by

$$\dot{Q}_t = \dot{Q}_b + \dot{Q}_m = \sum_i \Delta\dot{Q}_{b,i} H(t - t_i) + \sum_j A_p(t_j)\dot{Q}''_m(t - t_j) + \int_0^{t-t_j} \dot{Q}''_m(t - t_j - \xi)\dot{A}_p d\xi \qquad [21]$$

The index *i* provides tracking of changes in the burner output, which is given as user input values. The index *j* provides tracking of changes in the phase of fire growth due to the coefficients *a, b, & c* changing or to "instantaneous" ignition of newly covered areas for step increases of the burner. The next step is to determine the heat release flux profile, $\dot{Q}''_m(t - t_j)$, as an analytic approximation to the cone calorimeter data so that an analytic Laplace solution is found for Equation [20]. Earlier, it was described as an exponential decay function:

$$\dot{Q}''_m(t - t_j) = \dot{Q}''_{m,ig} H(t - t_j)\exp(-\omega_m (t - t_j)) \qquad [22]$$

Substitution of Equation [22] into Equation [21] and setting $t^* = t - t_j > 0$, the solution by the Laplace transform gives the result for the pyrolysis area and RHR in the recursive form as

$$A_p = \left(\frac{a + c(\dot{Q}_{mj} - A_{pj}\dot{Q}''_{m,iq} + \dot{Q}_{bj})}{\tau_m} + A_{pj}\omega_m\right)\left(\frac{\exp(s_1 t^*) - \exp(s_2 t^*)}{s_1 - s_2}\right)$$
$$+ \frac{c}{\tau_m}\sum_{t_i > t_j}\Delta\dot{Q}_{bj}H(t^* - t_i^*)\left(\frac{\exp(s_1(t^* - t_i^*)) - \exp(s_2(t^* - t_i^*))}{s_1 - s_2}\right)$$
$$+ \frac{c}{\tau_m}\sum_{t_i > t_j}\Delta\dot{Q}_{bj}H(t^* - t_i^*)\left(\frac{\omega_m}{s_1 - s_2}\right)\left(\frac{\exp(s_1(t^* - t_i^*)) - 1}{s_1} - \frac{\exp(s_2(t^* - t_i^*)) - 1}{s_2}\right) \quad [23]$$
$$+ \left(\frac{a + c\dot{Q}_{bj}}{\tau_m}\right)\left(\frac{\omega_m}{s_1 - s_2}\right)\left(\frac{\exp(s_1 t^*) - 1}{s_1} - \frac{\exp(s_2 t^*) - 1}{s_2}\right) + A_{pj}\left(\frac{s_1\exp(s_1 t^*) - s_2\exp(s_2 t^*)}{s_1 - s_2}\right)$$

$$\dot{Q}_t = \dot{Q}_{bj} + \left(\frac{(a + c\dot{Q}_{bj})\dot{Q}''_{m,ig} - b(\dot{Q}_{mj} - A_{pj}\dot{Q}''_{m,ig})}{\tau_m}\right)\left(\frac{\exp(s_1 t^*) - \exp(s_2 t^*)}{s_1 - s_2}\right)$$
$$+ \sum_{t_i > t_j}\Delta\dot{Q}_{bj}H(t^* - t_i^*) + \frac{c\dot{Q}''_{m,ig}}{\tau_m}\sum_{t_i > t_j}\Delta\dot{Q}_{bj}H(t^* - t_i^*)\left(\frac{\exp(s_1(t^* - t_i^*)) - \exp(s_2(t^* - t_i^*))}{s_1 - s_2}\right) \quad [24]$$
$$+ \dot{Q}_{pj}\left(\frac{s_1\exp(s_1 t^*) - s_2\exp(s_2 t^*)}{s_1 - s_2}\right)$$

where for brevity, we define $A_{pj} = A_{ig,j} + A_p(t_j)$, $\dot{Q}_{bj} = \dot{Q}_b(t_j)$, $\dot{Q}_{mj} = \dot{Q}''_{m,ig}A_{ig,j} + \dot{Q}_m(t_j)$, and

$$s_k = \frac{b + c\dot{Q}''_{m,ig} - \omega_m\tau_m}{2\tau_m} - (-1)^k\sqrt{\left(\frac{b + c\dot{Q}''_{m,ig} - \omega_m\tau_m}{2\tau_m}\right)^2 - \frac{b\omega_m}{\tau_m}} \quad [25]$$

Equation [25] involves complex numbers, which means the above solutions are considered to be in the complex variable domain. Specialized computer algorithms were developed for complex evaluations so that the above functions could be programmed directly.

Rate of Heat Release of Materials and Effect of Instrument Response

It is well known that the gas mixing in the gas flow train can make the peak rate of heat release flux (PRHR) appear significantly flattened. Thus, the flattening of PRHR with the profile of Equation [22] is given by a Duhamel convolution with the cone calorimeter's gas system response function as

$$\dot{Q}''_{m,cone} = \dot{Q}''_m \otimes \dot{S}_c = \dot{Q}''_{m,ig}\left(\frac{\exp(-\omega_m(t - t_j)) - \exp(-(t - t_j)/\tau_c)}{1 - \omega_m\tau_c}\right) \quad [26]$$

The total heat release flux (THR) is the integral of Equation [26], $THR = Q''_{m,ig}/\omega_m$, and PRHR is the local maximum value of Equation [26]. Since previous measurements have $\tau_c = 9.3$ seconds, the THR and PRHR are used as inputs to derive values for $Q''_{m,ig}$/ and ω_m. As a further validity, Equation [26] reproduced the ramp behavior of RHR immediately following ignition for most materials tested in the cone calorimeter.

For all tested materials, the measured PRHR and THR were found approximately as linear functions of the cone heater flux[16] and their coefficients are listed in Table 2. To determine the appropriate cone flux level for use in the fire growth model, we considered the data from Rhodes[17] in which a small diameter fluxmeter was inserted through a PMMA sample (which has emissivity of unity) exposed to the cone heater flux of 50 kW/m^2. At this flux level, the PMMA flame is more than 20 cm high, which gives the flame emissivity[17] as 0.09. Under these conditions, the fluxmeter has the value 77 kW/m^2. From Dietenberger[15], we used the convective heat transfer coefficient calibrated for the horizontal

position of specimen as h_C = 0.01433 + 1.33x10^{-4} kW / m^2K. From Janssens[14], we find the view factor from the cone heater to a 3-mm-diameter fluxmeter is very nearly unity, and to a 100- by 100-mm specimen, the view facter is 0.9679. Using these assumptions, we obtained a flame temperature of 1154 K (by setting Eq. [1] equal to 77 minus 50 kW/m^2), which corresponds to a flame radiative flux of 9 kW/m^2 and a convective flux of 18 kW/m^2 on the fluxmeter. In recent tests with different wood materials, we placed a 0.6-mm thermocouple near the spark ignition position. Values of 1,075 to 1,225 K were measured whenever the thermocouple was immersed in a flame, which allows us to adopt the PMMA flame property values for wood products in the cone calorimeter environment. In the next step, the net flux on the PMMA surface must account for the reduction in the cone heater view-factor and for the setting of surface temperature to about 600 K for pyrolyzing PMMA instead of 298 K for the fluxmeter. This means the flame flux is reduced and radiation from the surface is increased such that the net heat flux is calculated as 62 kW/m^2, a reduction of 15 kW/m^2 from that measured with the fluxmeter and an increase of 12 kW/m^2 from that of the cone heater set point.

Similarly, by using Equation [1], the 55 kW/m^2 measured with a fluxmeter on the wall corresponds to a net flux of 44.5 kW/m^2 for the PMMA material at pyrolyzing temperatures (recall T_f = 1173 K, $\mathrm{e}f$ = 0395, and h_C = 0.0165 kW / m^2K for propane burner). Using the procedure in the previous paragraph, the cone heater flux would have had to be set at 33 kW/m^2 to produce a net flux of 44.5 kW/m^2 on the burning PMMA specimen and thus also achieve the same level of heat release flux expected in the room test. Other materials gave similar results for the required cone flux levels.

Since the measurement of RHR for the room tests is based on the oxygen consumption method (see ISO9705), similar to the cone calorimeter, the consideration of gas flow train affecting the time response of RHR also applies. With a formula like Equation [26], the gas profiles responding to changes in the calibration gases for oxygen, carbon dioxide, and carbon monoxide are most consistent with the time constant, τ_g = 10 sec. Thus, a low-pass digital filter with a time constant of 10 seconds is applied to the signal from the electronic mass flow device for propane flow. Although the mass flow rate signal is already quite smooth, it is a quick response signal that needs filtering to mimic the time response of the gas analysis system. The filtered signal is then multiplied by the heat of combustion of propane. The resulting RHR is found to be in close agreement with the RHR from the oxygen consumption method even during step changes in the burner output.

For the case of the burner in the test room corner, the mixing of combustion products in the upper gas layer adds an effective time constant to the gas concentrations escaping out the doorway to the hood. We derived the upper-gas-layer time constant as τ_{room} = 18 sec, by applying a second low-pass digital filter to the filtered signal of propane mass flow rate, multiplying by the heat of combustion and matching the result with the RHR from the oxygen consumption method. Thus, without a submodel for the gas mixing in the upper hot gas layer, a double low-pass filter with time constants of 10 and 18 seconds should be applied to the model predictions to compare with the room test results. The analytical equivalent for the analytical fire growth model is the double application of the Duhamel's integral to Equation [24] as

$$\dot{Q}_{test} = \dot{Q}_t \otimes \dot{S}_g \otimes \dot{S}_{room} \qquad [27]$$

Simplicity of the model is maintained using the following generic substitutions in Equation [27]:

$$\exp(s_i t^*) \otimes \dot{S}_1 \otimes \dot{S}_2 = \left(\frac{\tau_1 \exp(-t^*/\tau_1)}{(\tau_2 - \tau_1)(1 + s_i\tau_1)} + \frac{\tau_2 \exp(-t^*/\tau_2)}{(\tau_1 - \tau_2)(1 + s_i\tau_2)} + \frac{\exp(s_i t^*)}{(1 + s_i\tau_1)(1 + s_i\tau_2)} \right) \qquad [28]$$

Empirical Relationships to Predict Lateral Flame Spread

At some critical time of fire growth, the RHR will change direction when upward flame spreading is exhausted. This occurs when the pyrolysis area reaches a critical level given by

$$A_{p,cr} = 1.7 A_{fu} \quad [29]$$

This is equivalent to a critical lateral spread of the pyrolysis region at the ceiling with an extension length slightly greater than the width of the burner. At the critical time, it is expected that the nature of flame extension on the ceiling will change the coefficients *a, b,* & *c*, which will require a solution restart. The simplest change is to modify the parameter, c_f, which is the ratio of flame extension length over the imposed flux profile characteristic length. For further simplification, we only considered the materials that flashed over during the 100-kW output of the burner. This left us with eleven materials, none of which had fire-retardant treatment (FRT). Six of these eleven materials correlated well with the value $c_f = 15$ and are the materials with a constant or decreasing RHR during the lateral flame spread phase. See Figures 1 and 2 for Tests 3, 5, 9, 12, 14, and 16. The pyrolysis area continuously increases while the RHR is decreasing. Because of the order of magnitude increase in the value of c_f, it was assumed that the dominant process is lateral flame spread in opposed flow. For the remaining five materials, it was also necessary to go back to Equation [15] and change the derivative to a different constant $dA_f / dQ_t = 0.011\ m^2/kW$. *This* is also the value consistent with experimental data obtained for flame spread with assisting flow, such as that in the Steiner tunnel (ASTM E84). The c_f in this case correlated best with the value 5. These five materials correspond to Tests 10, 11, 13, 17, and 18, and all of them had continuously rising RHR to flashover. For a clear demarcation into two groups of lateral flame spread, the product of time to ignition and total heat release flux is used to define a switching function as

$$1 / F_{sw} = 1 + 1.1671 * 10^6 * (t_{ig} * THR)^{(-20)} \quad [30]$$

so it can be used in the following functions:

$$c_f = 5F_{sw} + 15(1 - F_{sw}) \quad [31]$$

$$\frac{dA_f}{d\dot{Q}_t} = 0.011F_{sw} + 0.0051(1 - F_{sw}) \quad [32]$$

Thus, materials in the first group with low enough values of time to ignition or total heat release flux will have a relatively slow lateral flame spreading and result in a high value of time to flashover compared with materials in the second group. It seems contradictory that as ignition time is decreased, the time to flashover will increase. To clarify this, we note that within a group, a decrease in the time to ignition will also decrease the time to flashover. It is in the ability to go from a group of materials associated with fast flame spread to a group associated with slow flame spread that a decrease in time to ignition would achieve a higher time to flashover.

To complete the model, the criteria for the transition to downward flame spread is needed so that the fire growth solution can be restarted with the new coefficients. Using the pyrolysis area or any other single parameter generally did not succeed as a candidate criteria. However, an empirical relationship was found to relate the time at the transition of lateral to downward flame spread as a function of time, RHR and pyrolysis area at the transition points as

$$t_3 = 1.5\, t_2 + \left(\frac{A_{p3}}{0.00431\dot{Q}_{t3}} - 1 \right) \left[\frac{A_{p2}}{\dot{Q}_{t2}} \left(1 + \left| \frac{A_{p3}}{0.0154\dot{Q}_{t3}} - 1 \right|^{2.54} \right) \right]^{-1} \quad [33]$$

With this function, we focus only on the fire growth characteristics. For materials with FRT, there are only three tests in which it is not really possible to develop empirical relationships. Thus, they are modeled on a case by case basis with a view towards demonstrating features of the model.

RESULTS AND CONCLUSION

Our analytical model to predict flame spread and RHR for an ISO9705 test scenario contains many features that are critically lacking in similar models. The most significant example is the explicit inclusion of instrument responses into the model's prediction of RHR. With the oxygen consumption method providing the measurements of RHR, the model accounts for the room upper-gas-layer mixing using a time constant of 18 seconds and for the dead air mixing in the gas analyzing system using a time constant of 10 seconds. Figures 1 and 2 show the dotted curves predicted by the model that represents true RHR, Q_t, rather than the "measured" RHR, Q_{test}. The initial growth of pyrolysis areas has similar profiles to the true RHR but will continue to monotonically increase when the true RHR eventually peaks and decays. If the time responses of the gas flow train suddenly vanish during a test, the expected RHR at the derived flashover times range from 1,500 to 3,500 kW (Table 3). Since it is not possible to eliminate gas mixing in the upper gas layer of the room, suppose just the time constant for gas sampling system suddenly vanished. Then the expected RHR at the derived flashover times for the tests ranges from 740 to 1,210 kW. Thus, an RHR criteria of 1,000 kW for the flashover event may find agreement with a highly developed model of fire growth[5] but not with the room test data in various laboratories. As a result, different laboratories will not be able to agree on the RHR flashover criteria because each has inherently different time response for upper-gas-layer mixing and gas analyzing system. For the FPL room tests, the RHR at fkshover is 600 kW, while other laboratories have reported 1 MW at flashover. Using the criteria of 600 kW with "measured" RHR Q_{test}, we derived the times to flashover for the eleven materials without FRT (Table 3). The modeled values for time to flashover agree with the observed values within 1.2 percent standard deviation and are valid only for the untreated wood products in a single fire growth scenario.

Another instrument response often not considered is the time profile of the burner's heat flux on the wall. Laboratories will have inherently different setups for the propane gas delivery and this leads to different results on time to ignition of the wall specimen. With our electronic mass flow controller close to the test room, we derived a delay of one second to time of ignition for FPL room tests.

Table 3. RHR at time to flashover for different room and gas time constants for non-FRT materials

Material	Test No.	Observed flashover time at 600 kW (s)	Modeled flashover time at 600 kW (s)	Modeled RHR at flashover time for all time constants vanished (kW)	Modeled RHR at flashover time for gas time constant vanished (kW)
Oak veneer plywood	3	165	162	3,508	1,168
Douglas-fir plywood (ASTM)	5	474	466	2,711	1,131
Douglas-fir plywood (MB)	9	540	534	2,623	1,191
Southern Pine plywood	10	327	285	2,154	1,045
Particleboard	11	210	207	1,536	768
Oriented strandboard	12	168	179	2,787	1,207
Hardboard	13	228	221	1,683	839
Redwood lumber	14	504	505	2,574	1,092
White spruce lumber	16	600	600	1,863	739
Southern Pine boards	17	237	241	1,580	790
Waferboard	18	138	157	1,911	806

Our use of cone calorimeter data to derive material properties has significant advancements. First, materials with very low THR, such as rigid polyurethane foam, have their actual peak value of RHR about doubled the observed PRHR because of the 9 seconds for the time constant of the gas analyzing system. Next, we used an advanced ignitability analysis to report material properties of heat capacity, thermal conductivity, surface emissivity, and surface temperature at ignition for each tested material. Thus, unreasonable values for material properties derived for heavy and thin wood products with the

former thermally thick method were avoided. Lastly, using PMMA as an example, we derived that a cone flux of 33 kW/m^2 instead of 55 kW/m^2 is required to properly define the material's RHR for use in the fire growth model. The correct cone flux corresponds to the net heat flux from the burner flame on the burning wall material as being the same as that on the same burning material in the cone calorimeter. These advancements to using cone calorimeter data provide more reasonable properties for the tested materials.

The upward flame flux profile, as measured with fluxmeters, is a well-known nonlinear function of a burner's width and RHR. An appropriate linear approximation to the nonlinear function resulted in an exact Laplace solution to RHR and pyrolysis area and predicted well the upward fire growth of all tested materials. No similar correlation exists for the flame flux profile in the lateral direction. Thus, empirical modification to one or two coefficients for the upward flame flux profile seemed sufficient to predict lateral fire growth and to show that two groups of untreated flammable materials exist. The first group is described as continuously increasing RHR along with accelerating flame spread. These tend to be associated with high values of THR and time to ignitions, as with the heavy composite boards. The second group could be described as constant or decreasing RHR while in a slow lateral flame spreading mode. Plywood and lumber are in this second group.

The last group of materials tested consisted of three materials with FRT and the gypsum board. The results with the model show that a sudden increase in ignited area of 2.9 m^2 at the time of the burner's step increase from 100 to 300 kW corresponds to the peak value of RHR attained for the four tested materials. Although it is possible to specify a multistep burner profile in the current model by user input (and it is even set up to simulate all four scenarios of fire growth allowed in ISO 9705), the degree of empiricism required in the current model still prevents a valid general application.

NOMENCLATURE

A Area, m^2
a, b, c Fire growth coefficients, Equation [20]
$c_f = (y_f - y_c) / \delta_f$
C_p Heat capacity, J/Kg
$F_{dx-\ell}$ Viewfactor defined in Equation [18]
F_{sw} Switching function defined in Equation [30]
H Heavyside function
h Heat transfer coefficient, kW/Km^2
k Thermal conductivity, kW/Km
$\dot{Q}$ Rate of heat release (RHR), kW
$\dot{q}''$ Heat flux, kW/m^2
S Exponential response, Equation [4]
s_k Singularities of inverse transform of Eq. [20]
T Temperature, K
t time, s
v_p Pyrolysis front speed, m/s
w Burner width, m
y Surface distance, m
δ Feature dimension, m
ε Emissivity of radiation
ℓ Width of radiating plane, Equation [18], m
ρ Material density, kg/m^3
σ Stefan-Boltzmann constant, 5.67e-11 kW/K^{4}m^2
τ Time constant, s
ω Exponential time decay coefficient, 1/s

Subscript Definitions

b Propane ignition burner
c Cone calorimeter (convection when with h)
e Fluxmeter (radiant exposure, no flames)
f Flames adjacent to material
g Gas flow to analyzers
ig Ignition condition
m Material property or condition
p Pyrolyzing condition
s Surface of material or fluxmeter
w Wall of the room

ACKNOWLEDGMENTS

The authors thank the joint board of the Slovak-U.S. Science and Technology Program for financial support of the work presented in this paper under project number 94072.

REFERENCES

[1] Wickstrom, Ulf and Goransson, Ulf, 1992, Fire and Materials, Vol. 16, p. 15-22.
[2] Karlsson, Bjorn, 1993, Fire Safety Journal, vol. 20, p. 93-113.
[3] Saito, K, Quintiere, J.G., and Williams, F.A., 1985, Proceedings of the 1st International Symposium on Fire Safety Science, Gaithersburg, MD.
[4] Dietenberger, M., Grexa, O., White, R., Sweet, M. and Janssens, M. 1995, Proceedings for Fire & Materials 4th Int. Conf. and Exhibition, November 1995, Crystal City, VA, p. 53-62.
[5] Yan, Z. and Holmstedt, G., 1996, Fire Safety Journal, Vol. 27, p. 201-238.
[6] Quintiere, J., 1993, Fire Safety Journal, Vol. 20, p.313-339.
[7] Janssens, M., Grexa, O., Dietenberger, M., and White, R., 1995, Proceedings for Fire & Materials Fourth International Conference and Exhibition, November 1995, Crystal City, VA, p. 73-83.
[8] Kokkala, M., and Heinila M., 1991, Project 5 of the EUROFIC fire research programme.
[9] Williamson, R.B., Revenaugh, A., and Mowrer, F.W., 1991, Proceedings of the 3rd International Symposium of Fire Safety Science, p. 657-666.
[10] Kulkarni, A.K., Brehob, E., Manohar, S., and Nair, R., 1994, NIST-GCR-94-638.
[11] Dietenberger, M.A., 1991, Piloted Ignition and Flame Spread on Composite Solid Fuels in Extreme Environments, Ph.D. Dissertation, University of Dayton.
[12] Hasemi, Y., and Tokunaga, T., 1984, Combustion Science and Technology, Vol. 40, p. 1-17.
[13] Janssens, M., and Tran, H., 1996, Proceedings of the 7th meeting of the Interagency Working Group on Fire and Materials (IWGFM-7), Cosponsored with Annual Conf. on Fire Research, Oct., 1996.
[14] Janssens, M.L., 1991, Fundamental Thermophysical Characteristic of Wood and their role in Enclosure Fire Growth, Ph.D. Dissertation, University of Gent (Belgium).
[15] Dietenberger, M., 1996, Proceedings of the Int. Conf. on Fire Safety, Vol. 22, p. 189-197.
[16] Grexa, O., Janssens, M., and White, R., 1995, Proceedings for Fire & Materials Fourth International Conference and Exhibition, November 1995, Crystal City, VA, p. 63-71.
[17] Rhodes, B.T., 1994, NISTGCR-95-664.

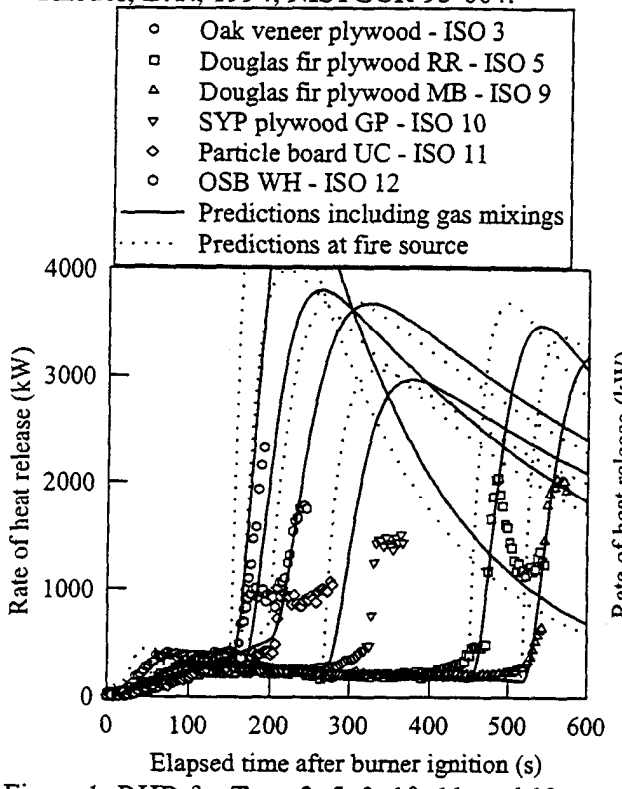

Figure 1: RHR for Tests 3, 5, 9, 10, 11, and 12.

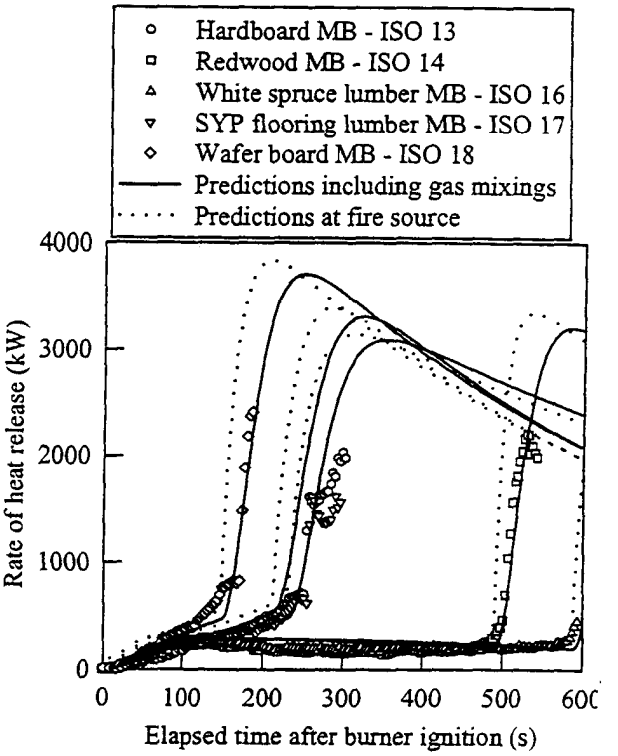

Figure 2: RHR for Tests 13, 14, 16, 17, and 18.

In: Proceedings of the fire and materials '99 --6th international conference and exhibition; 1999 February 22-23; San Antonio, TX. London, England: Interscience Communications Limited: 211-222